

**Statistical mechanics of passive Brownian particles in a fluctuating harmonic trap**Derek Frydel *Department of Chemistry, Universidad Técnica Federico Santa María, Campus San Joaquín, 8940897 Santiago, Chile*

(Received 20 April 2024; accepted 15 August 2024; published 29 August 2024)

We consider passive Brownian particles trapped in an “imperfect” harmonic trap. The trap is imperfect because it is randomly turned off and on, and as a result particles fail to equilibrate. Another way to think about this is to say that a harmonic trap is time dependent on account of its strength evolving stochastically in time. Particles in such a system are passive and activity arises through external control of a trapping potential, thus, no internal energy is used to power particle motion. A stationary Fokker-Planck equation of this system can be represented as a third-order differential equation, and its solution, a stationary distribution, can be represented as a superposition of Gaussian distributions for different strengths of a harmonic trap. This permits us to interpret a stationary system as a system in equilibrium with quenched disorder.

DOI: [10.1103/PhysRevE.110.024613](https://doi.org/10.1103/PhysRevE.110.024613)**I. INTRODUCTION**

A typical active particle system consists of particles that derive motion from an internal energy source. Standard models that represent such particles are the run-and-tumble (RTP) [1–16] and active-Brownian particle models [17,18], one more suitable to biological and the other to chemical systems. Another active scenario arises when a passive Brownian particle is immersed in a bath of active particles. The model that addresses this situation is the active Ornstein-Uhlenbeck particle model [19–24].

A different and somewhat less explored design of active dynamics is realized by placing passive Brownian particles in a fluctuating external potential, thereby preventing particles from equilibrating [25–30]. In this setup, there is no need for a special type of particles and the only requirement is that an external potential varies stochastically in time. A possible experimental realization of such a system could be attained using tweezer instruments and techniques [31–36].

This work considers passive Brownian particles trapped in a harmonic potential  $u = Kr^2/2$  with time-dependent strength  $K \equiv K(t)$ . We consider a specific evolution in which  $K(t)$  changes discontinuously between two discrete values, so the trap is either in an off or on state. The amount of time a particle spends in each state is drawn from an exponential distribution.

A stationary state of this system is governed by a third-order differential equation. A third-order differential equation were previously found to describe a stationary state of run-and-tumble particles in a static harmonic trap in one and two dimensions [37–39], for which a solution was found to be a convolution between two distributions. A stationary solution of the present system can be represented as a superposition of Gaussian distributions for different strengths of a harmonic trap. This permits us to interpret a stationary state as a system in equilibrium with quenched disorder. The superposition of Gaussian distributions has been encountered in quantum theory and financial markets [40,41]. In nonequilibrium statistical mechanics, those distributions have been considered in Ref. [42] in the context of nonextensive statistical mechanics.

The current work could be viewed in relation to systems that explore control of external forces and information feedback to perform work [43–50]. Although the model that is analyzed does not involve information feedback and the only control comes from regulating the time duration when particles are either trapped or released, it could be considered a small step in theoretical understanding of this class of problems.

Previous work done on systems with fluctuating external potentials include the study of particles in a harmonic trap with a fluctuating trap center [25] and that was motivated by an experiment [51]. A system of particles trapped in a harmonic trap with a fluctuating strength was first investigated in Ref. [27]. Particles in a fluctuating linear potential were investigated in Refs. [28,29] as a species of a resetting problem. The entropy production rate of single particle inside a fluctuating external potential of an arbitrary shape was calculated in Ref. [30].

This work is organized as follows. In Sec. II we introduce the model and obtain a third-order differential equation for a stationary state. In Sec. III we represent the solution as a superposition of Gaussian distributions for different trap strengths. In Sec. IV we consider particles trapped in a harmonic potential with a general time-dependent trap strength. It is shown that the time-dependent distribution at any given moment is a Gaussian distribution. This result justifies the use of the superposition formula. In Sec. V we extend all the exact results to a system for an arbitrary dimension. In Sec. VI we consider quantities of physical interest. The work is concluded in Sec. VII.

**II. THE MODEL**

The focus of this work is a conceptually simple model: an ideal gas trapped in an “imperfect” harmonic potential. The potential is imperfect because it is turned off and on at random time intervals. The alternate cycle of trapping and releasing prevents particles from attaining equilibrium and as a result gives rise to a nonequilibrium situation. The times  $t_p$  during

which a particle is either trapped or released are sampled from the exponential distribution  $\sim e^{-t_p/\tau}$ , where  $\tau$  is the average time during which a particle persists in a given state. At the end of each time  $t_p$ , a particle switches to another state with probability one.

Since the times when a trap is either in the “on” or “off” state are sampled from the same distribution, the system spends on average the same amount of time in both states. What changes is the rate, given by  $\tau^{-1}$ , with which the trap fluctuates between the two states. The model represents a specific case of a harmonic potential  $u = Kr^2/2$  with the time-dependent strength  $K \equiv K(t)$ .

For a system in one dimension, the Fokker-Planck formulation that describes such a model might be written as

$$\begin{aligned}\dot{\rho}_+ &= \mu \left( \frac{K}{2} + \Delta \right) [x\rho_+]' + D\rho_+'' + \frac{1}{\tau}(\rho_- - \rho_+) \\ \dot{\rho}_- &= \mu \left( \frac{K}{2} - \Delta \right) [x\rho_-]' + D\rho_-'' + \frac{1}{\tau}(\rho_+ - \rho_-),\end{aligned}\quad (1)$$

where  $\mu$  is the mobility,  $D = \mu k_B T$  is the diffusion constant,  $T$  is the temperature, and  $k_B$  is the Boltzmann constant. To simplify the expressions, we use the dot notation to represent the time derivative,  $\dot{\rho}_+ \equiv \frac{\partial \rho_+}{\partial t}$ , and the prime notation to represent derivatives with respect to position,  $[x\rho_+]' \equiv \frac{\partial}{\partial x}[x\rho_+]$  and  $\rho_+'' \equiv \frac{\partial^2}{\partial x^2} \rho_+$ .  $\rho_+$  and  $\rho_-$  are the distributions of particles in a harmonic potential with the respective strength  $K/2 + \Delta$  and  $K/2 - \Delta$ . The last term on the right-hand side of each equation represents the conversion of one type of particle into another and provides coupling between the two equations. The remaining terms represent the usual flux given by

$$j_{\pm} = -\mu(K/2 \pm \Delta)x\rho_{\pm} - D\rho_{\pm}'.$$

In this work we are interested in the situation  $\Delta = K/2$ , in which case the Fokker-Planck equation becomes [27]

$$\begin{aligned}\dot{\rho}_+ &= \mu K[x\rho_+]' + D\rho_+'' + \frac{1}{\tau}(\rho_- - \rho_+) \\ \dot{\rho}_- &= D\rho_-'' + \frac{1}{\tau}(\rho_+ - \rho_-).\end{aligned}\quad (2)$$

The distribution  $\rho_-$  represents unconstrained particles corresponding to the trap being turned off and  $\rho_+$  represents particles subject to a confining potential.

To simplify the notation, we introduce dimensionless parameters. The position of particles on the  $x$  axis and the rate at which a harmonic trap fluctuates in dimensionless units are given by

$$z = x\sqrt{\frac{\mu K}{D}}, \quad \alpha = \frac{1}{\tau\mu K}.$$

At a stationary state and dimensionless parameters Eq. (2) becomes

$$\begin{aligned}0 &= [z\rho_+]' + \rho_+'' + \alpha(\rho_- - \rho_+) \\ 0 &= \rho_-'' + \alpha(\rho_+ - \rho_-).\end{aligned}\quad (3)$$

The two equations can be merged into a single differential equation for a distribution  $\rho = (\rho_+ + \rho_-)/2$ . The result is a

third-order differential equation,

$$0 = -\alpha z^3 \rho + 2(1 - \alpha z^2)\rho' - (2 - z^2)z\rho'' + z^2\rho'''. \quad (4)$$

See Appendix A for details.

In the limit of a fast appearing-disappearing trap,  $\alpha \rightarrow \infty$ , Eq. (4) reduces to

$$0 = -\frac{z\rho}{2} - \rho', \quad (5)$$

where  $\rho$  is a Gaussian function  $\sim e^{-z^2/4}$ , which can be identified with passive particles in equilibrium but in a harmonic trap that is half the strength of the original trap.

Finding a solution to Eq. (4) for an arbitrary  $\alpha$  is more challenging. While first- and second-order differential equations are relatively common in physics, third-order differential equations are encountered less frequently [52]. They are also more challenging to solve and analyze. It is relatively easy, however, to analyze Eq. (4) by considering its moments.

The moments of a stationary distribution  $\rho$  can be obtained by transforming Eq. (4) into a recurrence relation by operating on it with  $\int_{-\infty}^{\infty} dz z^{2n-3}$  [37–39]. Followed by the integration by parts this yields

$$m_n = \frac{4n-2}{\alpha}[(n+\alpha)m_{n-1} - n(2n-3)m_{n-2}], \quad (6)$$

where  $m_n = \langle z^{2n} \rangle$  are even moments of  $\rho$ , all odd moments being zero.

Given the initial condition  $m_0 = 1$ , all subsequent moments can be calculated, and the first two terms of the sequence are

$$\begin{aligned}\langle z^2 \rangle &= \left( 2 + \frac{1}{\alpha} \right) \\ \langle z^4 \rangle &= 6 \left( 2 + \frac{3}{\alpha} + \frac{2}{\alpha^2} \right).\end{aligned}\quad (7)$$

In the limit  $\alpha \rightarrow \infty$ , all the moments reduce to the moments of a Gaussian distribution  $\sim e^{-z^2/4}$ . The moments increase as  $\alpha$  decreases, indicating the spreading out of  $\rho$ .

Moments of distributions corresponding do a different state can be calculated by operating on the two equations in Eq. (3) with  $\int dz z^{2n+2}$ . After some manipulation, the details of which can be found in Appendix B, we get two coupled recurrence relations, from which we get

$$\begin{aligned}\langle z^2 \rangle_+ &= 2 \\ \langle z^4 \rangle_+ &= 6 \left( 2 + \frac{1}{\alpha} \right),\end{aligned}\quad (8)$$

for particles in a trapped state, and

$$\begin{aligned}\langle z^2 \rangle_- &= 2 \left( 1 + \frac{1}{\alpha} \right) \\ \langle z^4 \rangle_- &= 6 \left( 2 + \frac{5}{\alpha} + \frac{4}{\alpha^2} \right),\end{aligned}\quad (9)$$

for particles in a released state. An interesting observation is that the second moment of trapped particles does not depend on  $\alpha$ ,  $\langle z^2 \rangle_+ = 2$ . This feature of a system will have interesting repercussions on various physical quantities discussed later in this work.

### III. SOLUTION AS A SUPERPOSITION OF GAUSSIAN DISTRIBUTIONS

In this section we develop a method that would permit us to solve a third-order differential equation in Eq. (4). As mentioned earlier, third-order differential equations are less common in physics. In the context of active particles, a third-order differential equation arises for RTP particles in a static harmonic trap in one and two dimensions [37]. For higher dimensions, a differential equation of the same system has a more complex structure and to date it was not possible to obtain it.

To solve Eq. (4) we represent  $\rho$  as a superposition of Gaussian distributions for different effective strengths,

$$\rho(z) = \int_0^1 d\lambda p(\lambda) \rho_G(z; \lambda), \quad (10)$$

where

$$\rho_G(z; \lambda) = \sqrt{\frac{\lambda}{2\pi}} e^{-\lambda z^2/2} \quad (11)$$

is a Gaussian distribution for a dimensionless strength  $\lambda$ . By representing the stationary distribution  $\rho$  as a superposition of equilibrium distributions (since  $\rho_G$  is an equilibrium distribution for an effective strength  $\lambda$ ), we reinterpret our system as not out-of-equilibrium but as effectively at equilibrium with quenched disorder. Thus, whatever features of  $\rho$  that make it deviate from a Gaussian form can be attributed to quenched disorder.

Other than providing an alternative interpretation of the original system, there is a certain mathematical advantage of representing a stationary distribution as a superposition formula, as this shifts the task from finding  $\rho$  to that of finding  $p(\lambda)$ , where it is reasonable to assume that  $p$  is less complex than  $\rho$ .

We note that since  $p(\lambda)$  is normalized, it follows that  $\int_{-\infty}^{\infty} dz \rho = 1$ . Also,  $p(\lambda)$  is defined on  $\lambda \in [0, 1]$ , since contributions  $\lambda > 1$  are not physically meaningful given that the actual system switches between the states  $\lambda = 0$  and  $\lambda = 1$ . This means that the superposition should span a continuous region between those two states, since the distribution itself does not jump from one state to another but evolves between the two states in a continuous manner.

To proceed, we distinguish between distributions  $p_+(\lambda)$  and  $p_-(\lambda)$ , such that  $\rho_{\pm} = \int_0^1 d\lambda p_{\pm}(\lambda) \rho_G(z; \lambda)$ . We then infer a differential equation for each distribution from Eq. (3). We use the word ‘‘infer’’ intentionally as there is no standard technique for obtaining a differential equation for  $p_{\pm}$  from Eq. (3). Instead, one proceeds using a trial-and-error approach. The two differential equations determined by this procedure are

$$\begin{aligned} 0 &= \frac{\partial}{\partial \lambda} [\lambda(\lambda - 1)p_+] + \frac{\alpha}{2}(p_- - p_+) \\ 0 &= \frac{\partial}{\partial \lambda} [\lambda^2 p_-] + \frac{\alpha}{2}(p_+ - p_-). \end{aligned} \quad (12)$$

Operating on each of the above equations with  $\int_0^1 d\lambda \rho_G(z; \lambda)$  recovers Eq. (3), which confirms the accuracy of Eq. (12). What is important about the result in Eq. (12) is that both equations are of a lower order than Eq. (3). Merging the two

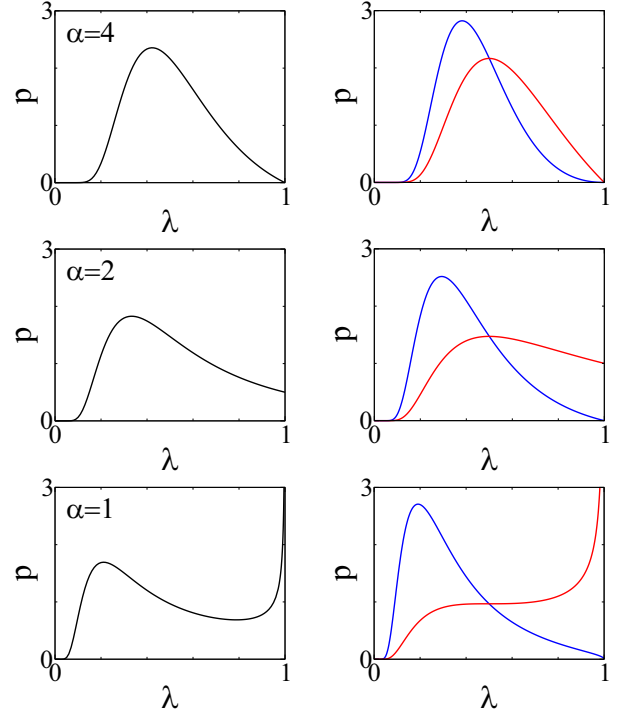


FIG. 1. Probability distribution  $p(\lambda)$  given in Eq. (14) for different values of  $\alpha$ . Distributions on the right-hand side column are for  $p_+$  and  $p_-$ . Blue distributions represent released particles  $p_-$  and red distributions represent trapped particles  $p_+$ .

equations in Eq. (12) leads to

$$0 = \left(3\lambda^2 - 2\lambda - \alpha\lambda + \frac{\alpha}{2}\right)p + (\lambda - 1)\lambda^2 p', \quad (13)$$

where  $p = (p_+ + p_-)/2$ . See Appendix (C) for details. Equation (13) is a first-order differential equation that can be easily solved. The solution is

$$p(\lambda) = \frac{1}{2} \frac{(\alpha/2)^{\alpha/2} e^{\alpha/2}}{\Gamma(\alpha/2)} \left(\frac{1}{\lambda} - 1\right)^{\frac{\alpha}{2}-1} \frac{e^{-\frac{\alpha}{2}\frac{1}{\lambda}}}{\lambda^3}, \quad (14)$$

and the solution for separate distributions  $p_{\pm}$  are

$$\begin{aligned} p_+ &= 2\lambda p \\ p_- &= 2(1 - \lambda)p, \end{aligned} \quad (15)$$

with  $p$  given in Eq. (14). Both solutions can be verified by inserting into Eq. (12).

Examining the expression in Eq. (14) we note that for  $\alpha = 2$  the factor  $(1/\lambda - 1)^{\frac{\alpha}{2}-1}$  reduces to unity, indicating some sort of crossover for this value of  $\alpha$ . To better see how this crossover manifests itself, in Fig. 1 we plot  $p(\lambda)$ , given in Eq. (14), for different values of  $\alpha$ . We recall that  $p(\lambda)$  is defined on  $\lambda \in [0, 1]$ , the reflection of the fact that the system fluctuates between the states  $\lambda = 0$  and  $\lambda = 1$ . The fact that  $p(0) = 0$  implies that the state  $\lambda = 0$  is inaccessible since for any finite  $\alpha$  particles remain confined to a finite region. To reach the state  $\lambda = 0$  the system would require an infinite amount of time.

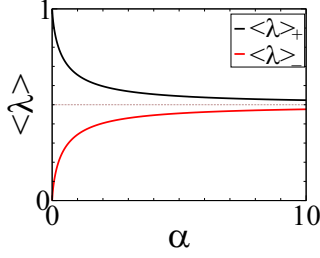


FIG. 2. The first moment of  $p_+(\lambda)$  and  $p_-(\lambda)$  as a function of  $\alpha$ .

The behavior at  $\lambda = 1$  is more interesting. The probability at  $\lambda = 1$  exhibits a crossover at  $\alpha = 2$  such that

$$p(1) = \begin{cases} 0 & \alpha > 2 \\ \frac{1}{2} & \alpha = 2. \\ \infty & \alpha < 2 \end{cases} \quad (16)$$

If fluctuations of a trap strength are rapid enough, such that  $\alpha > 2$ , then the state  $\lambda = 1$  is never attained and  $p(1) = 0$ . For a slower rate of fluctuations, such as  $\alpha < 2$ , particles remain trapped for a sufficiently long time. This permits a system to come very close to  $\lambda = 1$ , giving rise to a divergence at  $\lambda = 1$ . The divergence, however, is integrable, indicating that the state  $\lambda = 1$  is being approached but never truly attained.

Note that although we analyze a stationary distribution, we talk about a system as evolving between two states. The system is stationary when it is averaged over time, or over many independent ensembles. We will discuss the aspect of time dependence in more detail in Sec. IV.

Separate distributions  $p_{\pm}(\lambda)$  are displayed on the right-hand side in Fig. 1. The distributions  $p_+$  and  $p_-$  become increasingly similar with increasing  $\alpha$  and converge in the limit  $\alpha \rightarrow \infty$ . On the other hand, the two distributions become increasingly distinct as  $\alpha$  becomes smaller. The two distributions shift toward a different side of the domain and evolve into very different shapes. The released particles move toward the state  $\lambda = 0$  and the trapped particles concentrate around  $\lambda = 1$ .

Despite very different shapes, the first moment of each distribution, shown in Fig. 2, are symmetric around  $\lambda = 1/2$ , and as a result the average value of  $\lambda$  of the total distribution  $p = (p_+ + p_-)/2$  is fixed at  $\langle \lambda \rangle = \frac{1}{2}$  and is independent of  $\alpha$ . There is no symmetry between higher moments.

Using the superposition formula in Eq. (10) together with the formula for  $p(\lambda)$  in Eq. (14), the solution of the third-order differential equation in Eq. (4) can be expressed as

$$\rho(z) = \frac{(\alpha e/2)^{\alpha/2}}{2\Gamma(\alpha/2)} \left(\frac{1}{2\pi}\right)^{\frac{1}{2}} \int_0^1 d\lambda \left(\frac{1}{\lambda} - 1\right)^{\frac{\alpha}{2}-1} \frac{e^{-\frac{\alpha}{2\lambda}} e^{-\frac{\lambda z^2}{2}}}{\lambda^{3-\frac{1}{2}}}. \quad (17)$$

The integral in Eq. (17) can be evaluated exactly for specific values of  $\alpha$  corresponding to  $\alpha = 2n$  where  $n$  is the positive integer [27]. For  $\alpha = 2$ , which according to Eq. (16) corresponds to a crossover, the term  $(\frac{1}{\lambda} - 1)^{\frac{\alpha}{2}-1}$  in Eq. (17) becomes unity and  $p(\lambda)$  evaluates to the following analytical

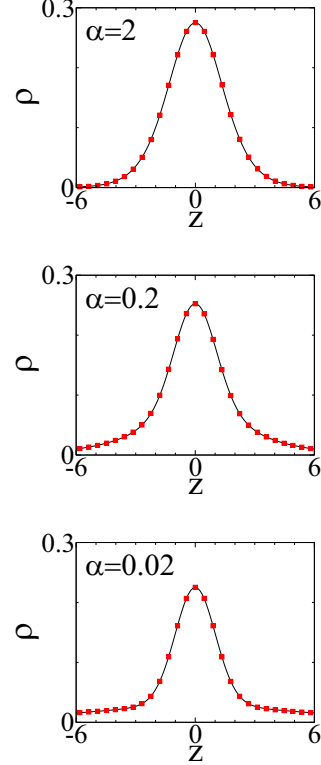


FIG. 3. Distributions  $\rho(z)$  calculated using Eq. (17) for different values of  $\alpha$ . Red data points are obtained from a simulation based on numerical integration of the Langevin equation.

form

$$\rho = \frac{1}{2} \frac{e^{-z^2/2}}{\sqrt{2\pi}} + \frac{1}{8\sqrt{2}} \left[ (1 - \sqrt{2z^2}) \operatorname{erfc} \left[ 1 + \frac{\sqrt{2z^2}}{2} \right] e^{1+\sqrt{2z^2}} \right] + \frac{1}{8\sqrt{2}} \left[ (1 + \sqrt{2z^2}) \operatorname{erfc} \left[ 1 - \frac{\sqrt{2z^2}}{2} \right] e^{1-\sqrt{2z^2}} \right]. \quad (18)$$

In Fig. 3 we plot  $\rho(z)$  for different values of  $\alpha$ . For those values of  $\alpha$  where no analytical expression is available, the integral in Eq. (17) is evaluated numerically. All probability distributions are in addition compared with distributions obtained from simulation based on numerical integration of the Langevin equation to confirm the correctness of analytical results. The Langevin equation is integrated using the Euler method,

$$\begin{aligned} x_+(t + \Delta t) &= x_+(t) - \mu K x_+(t) + \xi_+(t) \sqrt{2D\Delta t} \\ x_-(t + \Delta t) &= x_-(t) + \xi_-(t) \sqrt{2D\Delta t}, \end{aligned} \quad (19)$$

where  $\xi_{\pm}(t)$  is the white noise with zero mean and unity variance and  $x_+$  and  $x_-$  is the position of a particle in a trapped and released state, respectively. An individual particle changes from  $x_+$  to  $x_-$  and vice versa at the end of the time  $t_p$  drawn from the exponential distribution  $\sim e^{-t_p/\tau}$ .

The primary non-Gaussian feature of the distributions is that particles spread out beyond the trap boundaries. This feature becomes more pronounced for small values of  $\alpha$  where particles are permitted to remain in a given state for a longer time. By allowing particles to be released for a longer time,

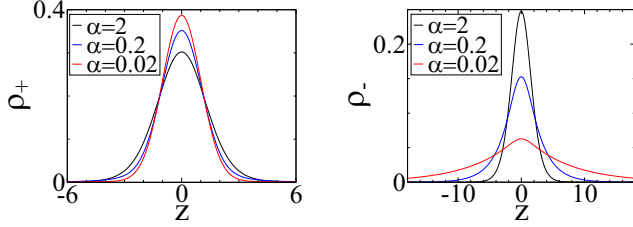


FIG. 4. Distributions of trapped and released particles,  $\rho_+$  and  $\rho_-$ , obtained from the superposition formula in Eq. (10) and the distributions  $p_{\pm}$  in Eq. (15) for different parameters  $\alpha$ .

distributions become more spread out. What is interesting is that we did not observe any distinct features in  $\rho$  that would signal the crossover at  $\alpha = 2$ . The crossover appears to be the feature of  $p(\lambda)$ .

We can get a better sense of what is happening by plotting distributions for separate states  $\rho_{\pm}$ . In Fig. 4 we plot distributions  $\rho_{\pm}$  calculated using the superposition formula in Eq. (10) and the distributions  $p_{\pm}$  in Eq. (15).

$\rho_+$  and  $\rho_-$  respond quite differently to the reduction of  $\alpha$ . While  $\rho_+$  converges to a Gaussian distribution for the strength  $\lambda = 1$ ,  $\rho_-$  becomes more spread out and deviates increasingly from a Gaussian form. Thus, the spread of particles seen in Fig. 3 is primarily attributed to released particles.

#### Characteristic function

Even though the integral in Eq. (17) cannot be evaluated for an arbitrary  $\alpha$ , the characteristic function  $\hat{\rho}(q) = \int_{-\infty}^{\infty} dz e^{-iqz} \rho(z)$  has a relatively simple algebraic form given by

$$\hat{\rho}(q) = e^{-q^2/2} \left[ \frac{2\alpha + q^2}{2\alpha} \left( \frac{\alpha}{\alpha + q^2} \right)^{\frac{\alpha}{2} + 1} \right]. \quad (20)$$

Since the factor  $e^{-q^2/2}$  is the characteristic function of the Boltzmann distribution, we can represent  $\hat{\rho}(q)$  as

$$\hat{\rho}(q) = \hat{\rho}_{\text{eq}}(q) \hat{\rho}_{\text{neq}}(q),$$

where  $\hat{\rho}_{\text{eq}}(q) = e^{-q^2/2}$  and  $\hat{\rho}_{\text{neq}}(q)$  captures nonequilibrium contributions. As the product of two Fourier transformed function corresponds to the convolution in the real space, we could represent  $\rho$  as

$$\rho(z) = \int dz' \rho_{\text{eq}}(z - z') \rho_{\text{neq}}(z'), \quad (21)$$

and because the convolution construction implies the presence of two independent random processes, we could interpret  $\rho_{\text{neq}}$  as some type of random process, although it is not clear how to identify such a process. At the crossover  $\alpha = 2$ ,  $\rho_{\text{neq}}$  is found to have a simple form given by

$$\rho_{\text{neq}} = \frac{e^{-|z|\sqrt{2}}}{8} (3\sqrt{2} + 2z), \quad (22)$$

and the convolution formula in Eq. (21) smears out this result into the formula in Eq. (18). Despite Gaussian smearing, the asymptotic behavior of  $\rho$  should be dominated by the

exponential form of  $\rho_{\text{neq}}$ , which indicates that  $\rho$  has different asymptotic behavior than that of a Boltzmann distribution.

#### IV. TIME-DEPENDENT HARMONIC TRAP

In this section we provide justification for the superposition formula in Eq. (10). The system we study is time dependent due to constant evolution of the trap strength over time. However, if we average this distribution over long times, we obtain a stationary distribution.

We start by considering a harmonic potential with a general time-dependent strength,

$$u(x, t) = \frac{K(t)x^2}{2}. \quad (23)$$

We next assume that the time-dependent distribution of such a system is a Gaussian function at all times,

$$\rho(x, t) = \sqrt{\frac{\mu K_{\text{eff}}}{2\pi D}} \exp\left[-\frac{\mu K_{\text{eff}} x^2}{D}\right], \quad (24)$$

where the only parameter that changes in time is the time-dependent effective strength  $K_{\text{eff}}(t)$  such that  $K_{\text{eff}}(t) \neq K(t)$  [unless  $K(t)$  varies very slowly]. The only constraint we introduce is that at  $t = 0$ ,  $\rho(x, t)$  is a Gaussian function corresponding to some initial effective strength  $K_0 = K_{\text{eff}}(0)$ .

To calculate  $K_{\text{eff}}$ , we insert the Gaussian distribution in Eq. (24) into the corresponding time-dependent Fokker-Planck equation,

$$\dot{\rho} = \mu K(t)[x\rho]' + D\nabla^2 \rho, \quad (25)$$

which yields the following equation:

$$\mu K - \mu K_{\text{eff}} = \frac{1}{2} \frac{d \ln K_{\text{eff}}}{dt}, \quad (26)$$

for which the solution is

$$K_{\text{eff}}(t) = \frac{K_0}{e^{-2 \int_0^t dt' \mu K(t')} + 2\mu K_0 \int_0^t dt' e^{-2 \int_0^{t'} dt'' \mu K(t'')}}. \quad (27)$$

The fact that Eq. (26) can be solved implies that the Gaussian distribution in Eq. (24) is a correct time-dependent distribution and the solution of Eq. (25).

If  $K(t)$  changes in some periodic, quasiperiodic, or any other repetitive fashion, then it should be possible to obtain a stationary distribution by averaging  $\rho$  over a long time,

$$\rho(x) = \lim_{t \rightarrow \infty} \frac{1}{t} \int_0^t dt' \rho(x, t'). \quad (28)$$

And since it was determined that the distribution at all times has a Gaussian form, we could alternatively represent  $\rho(x)$  as a superposition of Gaussian distributions,

$$\rho(x) = \lim_{t \rightarrow \infty} \frac{1}{t} \int_0^t dt' \rho_G(z, t') = \int_0^1 d\lambda p(\lambda) \rho_G(z; \lambda), \quad (29)$$

where the probability distribution  $p(\lambda)$  depends on a specific evolution of  $K_{\text{eff}}(t)$ . The superposition formula in Eq. (10) is simply a consequence of this relation.

In the case that  $K(t)$  changes discontinuously as  $K_0 \rightarrow K_1$ , Eq. (27) reduces to

$$K_{\text{eff}}(t) = \frac{K_0 K_1}{K_0 - (K_0 - K_1) e^{-2\mu K_1 t}}. \quad (30)$$

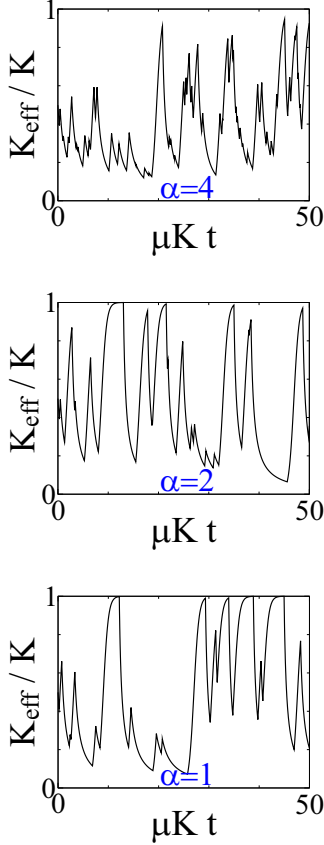


FIG. 5.  $K_{\text{eff}}$  of a fluctuating trap for different  $\alpha = 1/\mu K \tau$ . The initial value is  $K_{\text{eff}}(0) = K/2$  for all figures.

In the model considered in this work, the strength of the harmonic potential changes between two discrete values, 0 and  $K$ , corresponding to the strength of the actual trap.

Using Eq. (30), we could calculate the evolution of  $K_{\text{eff}}(t)$ , where  $K(t)$  fluctuates between two values and remains in each value for the stretch of time drawn from the exponential distribution. The resulting evolution of  $K_{\text{eff}}$  is shown in Fig. 5 for different values of  $\alpha$ .

For  $\alpha = 4$ , which is above the point of crossover,  $K_{\text{eff}}$  fails to come close to  $K$  due to rapid fluctuations of a trap. This explains why the probability distribution  $p(\lambda)$  in Fig. 1 for the same value of  $\alpha$  is zero at  $K_{\text{eff}}/K = \lambda = 1$ . For  $\alpha = 1$ , which is below the crossover,  $K_{\text{eff}}$  can approach  $K$  and then remain close to it for extended periods of time. This gives rise to a divergence in  $p(\lambda)$  at  $\lambda = 1$  seen in Fig. 1 for the same value of  $\alpha$ .

One can obtain the distribution  $p(\lambda)$  from the evolution of  $K_{\text{eff}}(t)$  using  $p(\lambda) \sim \lim_{t \rightarrow \infty} \frac{1}{t} \frac{dt}{d\lambda}$ , where  $\lambda(t) = K_{\text{eff}}(t)/K$ .

## V. EXTENSION TO HIGHER DIMENSIONS

It is rather straightforward to extend the results in Sec. IV to an arbitrary dimension  $d$ . Given a time-dependent harmonic potential,

$$u(r, t) = \frac{K(t)r^2}{2}, \quad (31)$$

where  $r^2 = \sum_{i=1}^d x_i^2$  is the radial distance from a trap center for a system in dimension  $d$ . We next assume that the time-dependent distribution has a Gaussian form at all times,

$$\rho(r, t) = \left( \frac{\mu K_{\text{eff}}}{2\pi D} \right)^{d/2} \exp \left[ -\frac{\mu K_{\text{eff}}}{D} \frac{r^2}{2} \right]. \quad (32)$$

To obtain an expression for  $K_{\text{eff}}(t)$ , we insert the Gaussian distribution above into the corresponding Fokker-Planck equation,

$$\dot{\rho} = \mu K(t) \nabla \cdot (\mathbf{r} \rho) + D \nabla^2 \rho. \quad (33)$$

Such a procedure recovers the relation in Eq. (26) for which the solution is the expression in Eq. (27). This proves that  $K_{\text{eff}}(t)$  in Eq. (27) is valid for any dimension.

Other results in this work can also be extended to an arbitrary dimension. The Fokker-Planck equation for the fluctuating potential model, analogous to Eq. (2) but for an arbitrary dimension, is given by

$$\begin{aligned} \dot{\rho}_+ &= \mu K \nabla \cdot [\mathbf{r} \rho_+] + D \nabla^2 \rho_+ + \frac{1}{\tau} (\rho_- - \rho_+) \\ \dot{\rho}_- &= D \nabla^2 \rho_- - \frac{1}{\tau} (\rho_- - \rho_+). \end{aligned} \quad (34)$$

For a stationary state and in reduced units the two equations become

$$\begin{aligned} 0 &= \nabla \cdot [\mathbf{s} \rho_+] + \nabla^2 \rho_+ + \alpha (\rho_- - \rho_+) \\ 0 &= \nabla^2 \rho_- - \alpha (\rho_- - \rho_+), \end{aligned} \quad (35)$$

where  $\mathbf{s} = \mathbf{r} \sqrt{\frac{\mu K}{D}}$ .

The moments of stationary distributions can be obtained by operating on both equations in Eq. (35) with  $\int d\mathbf{r} r^{d-1} r^{2n}$ . The resulting expressions for the second moment are

$$\begin{aligned} \langle s^2 \rangle_+ &= 2d \\ \langle s^2 \rangle_- &= 2d \left( 1 + \frac{1}{\alpha} \right) \\ \langle s^2 \rangle &= d \left( 2 + \frac{1}{\alpha} \right). \end{aligned} \quad (36)$$

By combining the two equations in Eq. (35) we obtain a third-order differential equation,

$$\begin{aligned} 0 &= -\alpha s^3 \rho + [3 - d - (2\alpha + 1 - d)s^2] \rho' \\ &\quad - [3 - d - s^2] s \rho'' + s^2 \rho'''. \end{aligned} \quad (37)$$

Note that by setting  $d = 1$  we recover Eq. (4). To find the solution of the above equation, we represent a stationary distribution as a superposition of Gaussian distributions,

$$\rho(s) = \int_0^1 d\lambda p(\lambda) \rho_G(s; \lambda), \quad (38)$$

where

$$\rho_G(s; \lambda) = \left( \frac{\lambda}{2\pi} \right)^{d/2} e^{-\lambda s^2/2}. \quad (39)$$

Since it was determined that  $K_{\text{eff}}(t)$  is independent of  $d$ , and since it is possible to obtain the probability distribution

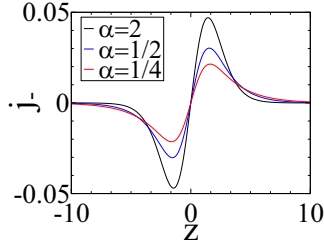


FIG. 6. Flux for particles released from the trap. Flux for particles in a trapped state, not shown in the figure, is  $j_+ = -j_-$ .

$\rho(\lambda)$  from the evolution of  $K_{\text{eff}}(t)$ , we conclude that the expression for  $\rho(\lambda)$  in Eq. (14) is valid for all  $d$ . This means that any dependence on  $d$  comes from the Gaussian distribution in Eq. (39), and the solution of the third-order differential equation in Eq. (37) is given by

$$\rho(s) = \frac{(\alpha e/2)^{\alpha/2}}{2\Gamma(\alpha/2)} \left(\frac{1}{2\pi}\right)^{\frac{d}{2}} \int_0^1 d\lambda \left(\frac{1}{\lambda} - 1\right)^{\frac{\alpha}{2}-1} \frac{e^{-\frac{\alpha}{2\lambda}} e^{-\frac{\lambda s^2}{2}}}{\lambda^{3-\frac{d}{2}}}. \quad (40)$$

We note that the solution is not limited to integer values of  $d$  and applies to any value of  $d$ .

## VI. QUANTITIES OF PHYSICAL INTEREST

### A. Potential energy

In this section we look into physical quantities of the model, starting with the average potential energy  $\langle u \rangle_{\pm} = K \langle r^2 \rangle_{\pm} / 2$ . Using the moments in Eq. (36), the potential energy for particles in each state is found to be

$$\begin{aligned} \langle u \rangle_+ &= dk_B T, \\ \langle u \rangle_- &= 0. \end{aligned} \quad (41)$$

The potential energy of particles in a released state is zero since the trap is switched off. Another interesting observation is that the potential energy of particles in a trapped state does not depend on the rate parameter  $\alpha$ . Adding the two contributions, the total potential energy is found to be the same as that for a system in equilibrium,

$$\langle u \rangle = \frac{dk_B T}{2}. \quad (42)$$

The fluctuating harmonic potential might considerably alter stationary distributions but the average potential energy is unaffected. The mathematics of this result can be traced to the fact that the second moment of trapped particles, see Eq. (36), does not depend on  $\alpha$ .

### B. Flux

We next consider flux, which for particles in each state and for  $d = 1$  is given by

$$j_- = -D\rho'_-, \quad j_+ = -\mu K x \rho_+ - D\rho'_+. \quad (43)$$

Also note that the total flux is zero everywhere,  $j = j_+ + j_- = 0$ .

In Fig. 6 we plot flux for particles in a released state,  $j_-$ , in dimensionless units given by  $j_-(z) = -\rho'_-(z)$ . (No insight is

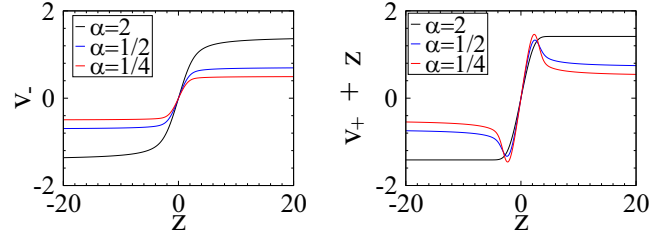


FIG. 7. Local velocity for different values of  $\alpha$ . For trapped particles we plot  $v_+ + z$  to subtract contributions of an external force, as a result, both quantities represent diffusional component of a local velocity. In both cases this corresponds to plotting  $-\ln \rho_{\pm}'$ .

gained by plotting  $j_+$  since  $j_+ = -j_-$ ). The first observation is that released particles move away from the trap center, which is expected because particles are released. The second observation is that the magnitude of the flux increases with increased  $\alpha$ . This makes sense since released particles tend to be more compressed when  $\alpha$  is large and so diffusion away from the trap center should be greater.

As both fluxes have the same functional form, a better insight could be gained by looking into the local velocity, in dimensionless units given by

$$v_+ = \frac{j_+}{\rho_+} = -[\ln \rho_+]' - z, \quad v_- = \frac{j_-}{\rho_-} = -[\ln \rho_-]'. \quad (44)$$

Note that the velocity in a trapped state has an additional linear term resulting from an external force. The other term in each expression comes from diffusion.

Local velocities are shown in Fig. 7. For particles in a trapped state we plot  $v_+ + z$  to subtract contributions of an external force. Consequently, the two plots amount to  $-\ln \rho_{\pm}'$  and represent diffusional component of a local velocity.

The most striking feature is that the local velocity does not vanish at infinity but saturate at a nonzero constant. Since the quantity that is plotted is  $-\ln \rho_{\pm}'$ , this implies that distributions  $\rho_{\pm}$  decay exponentially. Such an asymptotic behavior has been hinted at in Sec. III A and was proven for  $\alpha = 2$  in Eq. (22).

### C. Entropy production rate

One feature of an active system is that it generates heat that is dissipated into reservoir. In the case of active particles, it is the internal energy of a particle that is converted to heat. In the case of a present system, the heat is generated when the work done by an external potential to compress particles is converted to heat.

By measuring the rate of heat that is dissipated, we could quantify a distance of how far from equilibrium a system is, since the rate of heat dissipation,  $\langle \dot{q} \rangle$ , is related to the entropy production rate  $\Pi$  via the relation  $T\Pi \equiv \langle \dot{q} \rangle$ , where  $T$  is the temperature [53].

There are different ways one can obtain an expression for the entropy production rate [30]. Here we are going to follow an intuitive approach. A particle that is moving through a dissipating medium experiences the drag force  $\mathbf{F}_d = -\mu^{-1}\mathbf{v}$ , where  $\mathbf{v}$  is the velocity vector. An instantaneous rate of heat dissipation is then given by  $\dot{q} = \mu^{-1}v^2$ . However,

when calculating the average rate of heat dissipation, we need to subtract the equilibrium contributions,  $\langle \dot{q} \rangle = \mu^{-1} \langle v^2 \rangle - \mu^{-1} \langle v^2 \rangle_{\text{eq}}$ , since these contributions are not truly dissipated but are recovered at some point in time in the form of thermal fluctuations as a consequence of the fluctuation-dissipation relation. And since  $\langle v^2 \rangle_{\text{eq}} = dk_B T/m$ , we can write

$$\langle \dot{q} \rangle = \frac{1}{\mu} \left[ \langle v^2 \rangle - \frac{dD}{\tau_r} \right], \quad (45)$$

where  $\tau_r = m\mu$  is the inertial relaxation and  $m$  is the mass of a particle. For overdamped dynamics there is no inertia and  $\tau_r = 0$ .

To calculate the average velocity  $\langle v^2 \rangle$  we formulate our model in the underdamped regime. The formulation and subsequent derivations are carried out in Appendix D. Here we write down the end result,

$$\langle v^2 \rangle - \frac{dD}{\tau_r} = \frac{d\mu KD}{2} \frac{(1 + \tau_r/\tau)}{1 + 3\tau_r/\tau + \tau_r^2/\tau^2(2 - \mu K\tau/2)}, \quad (46)$$

and remind that  $\tau$  is the average time during which a system remains in a given state. Inserting the above expression in Eq. (45) yields

$$T\Pi \equiv \langle \dot{q} \rangle = \frac{dKD}{2} \frac{(1 + \tau_r/\tau)}{1 + 3\tau_r/\tau + \tau_r^2/\tau^2(2 - \mu K\tau/2)}. \quad (47)$$

For the overdamped regime  $\tau_r = 0$ , the expression above reduces to

$$T\Pi \equiv \langle \dot{q} \rangle = \frac{dDK}{2}. \quad (48)$$

The entropy production rate for a fluctuating harmonic trap in the overdamped regime has been previously obtained in Ref. [30]. Equation (48) is in agreement with that result.

The main difference between the result in Eq. (48) and the dissipation of heat of typical systems of active particles in a harmonic trap, such as run-and-tumble and active Brownian particles, is that  $\langle \dot{q} \rangle$  in these systems depends on  $\alpha$  as  $\langle \dot{q} \rangle \propto \alpha/(1 + \alpha)$  [53], where  $\alpha$  represents the rate at which an active particle changes direction of motion. According to this relation,  $\langle \dot{q} \rangle$  is maximal in the limit  $\alpha \rightarrow \infty$  and then decreases monotonically to zero as  $\alpha \rightarrow 0$ . The reason that  $\langle \dot{q} \rangle$  vanishes as  $\alpha \rightarrow 0$  is that the direction of motion in this limit changes very seldom and there is sufficient time for a system to attain equilibrium. In the current system, the attainment of equilibrium even in the limit  $\alpha \rightarrow 0$  is not possible—since for particles in a released state equilibrium corresponds to particles that are spread out into infinity. Attaining this distribution would require an infinite amount of time. As a result, particles in a fluctuating harmonic trap remain agitated even in the limit  $\alpha \rightarrow 0$ .

We next look into the formula for the dissipation of heat in the underdamped regime  $\tau_r > 0$  in Eq. (47). The first observation is that  $\langle \dot{q} \rangle$  is no longer independent of  $\tau$  (or  $\alpha = 1/\tau\mu K$ ). Even for cases where inertia is negligible but nonvanishing, and the formula in Eq. (48) accurately predicts the dissipation of heat for a significant range of  $\tau$ , the dependence on  $\tau$  becomes important in the limit  $\tau \rightarrow 0$  (or  $\alpha \rightarrow \infty$ ) where  $\langle \dot{q} \rangle$  is found to vanish. This is a drastically different limiting behavior than that deduced from the overdamped regime. Since the

vanishing dissipation of heat indicates equilibrium, it means that the system in the limit  $\alpha \rightarrow \infty$  is in equilibrium; however, we only reach this conclusion when we incorporate inertia into a theoretical description. Since underdamped dynamics represents a more complete description, we conclude that the limit  $\alpha \rightarrow \infty$  indeed represents a true equilibrium. This claim is supported by the fact that a stationary distribution in this limit converges to a Gaussian distribution, see Eq. (5).

## VII. CONCLUSION

This work considers an ideal gas confined to a harmonic trap  $u = Kr^2/2$  with time dependent strength  $K \equiv K(t)$ . It is demonstrated that the time dependent distribution of such a system  $\rho(x, t)$  has a Gaussian form at all times, corresponding to some effective strength of the harmonic potential,  $K_{\text{eff}}(t) \neq K(t)$ .

We are interested in a specific time evolution of  $K(t)$  such that it changes discontinuously between two discrete values, 0 and  $K$ , and where the time during which a trap remains in a given state is drawn from an exponential distribution  $\sim e^{-t_p/\tau}$ .

A stationary distribution of this system can be obtained from a third-order differential equation, the solution of which is represented as a superposition of Gaussian distributions for different strengths of a harmonic trap,  $\rho(x) = \int_0^K dK' p(K') \rho_G(x; K')$ . The reason for the superposition can be traced back to the fact that a time-dependent distribution at all times has a Gaussian form.

The probability distribution  $p(K)$  can be obtained and analyzed. The resulting algebraic expression for  $p(K)$  exhibits a crossover at  $\tau = 2/\mu K$ . For  $\tau > 2/\mu K$ , the distribution  $p(K')$  diverges at  $K' = K$ , indicating that a fraction of particles comes close to an equilibrium-like behavior. The divergence disappears for  $\tau < 2/\mu K$ . For very small  $\tau$ , a stationary distribution converges to a Gaussian form for a trap with the strength which is half the strength of the physical trap,  $K/2$ .

The primary feature of a resulting stationary distribution  $\rho(x) = \int_0^K dK' p(K') \rho_G(x; K')$  is the spread-out caused by the periods during which a trap is turned off. Since the period during which a trap is turned off increases with  $\tau$ , the distributions tend to be more spread out for larger  $\tau$ . The spreading component of distributions is dominated by an exponential decay.

The spreading-out feature of the current model is very different from the behavior of active particles. Active particles are known to accumulate near the trap boundaries rather than penetrate these boundaries [32,54]. For example, in the case of active particles trapped in a harmonic trap, the accumulation of particles at trap borders leads to bimodal stationary distributions, with excess of particles close to boundaries and depletion of particles near a trap center, [2,6,37]. These models exhibit crossover when a stationary distribution changes from a bimodal to unimodal distribution.

The data that support the findings of this study are available from the corresponding author on reasonable request.

## ACKNOWLEDGMENTS

D.F. acknowledges financial support from FONDECYT through Grant No. 1241694.

**APPENDIX A: DERIVATION OF EQ. (4)**

In this section we show how the two coupled differential equations in Eq. (3), which we reproduce below:

$$\begin{aligned} 0 &= [z\rho_+] + \rho_+'' + \alpha(\rho_- - \rho_+), \\ 0 &= \rho_-'' + \alpha(\rho_+ - \rho_-), \end{aligned} \quad (\text{A1})$$

are combined to yield a single differential equation in Eq. (4). The two equations can be either added or subtracted, where each procedure yields

$$\begin{aligned} 0 &= \frac{1}{2}[z\rho]' + \frac{1}{2}[z\sigma]' + \rho'', \\ 0 &= \frac{1}{2}[z\rho]' + \frac{1}{2}[z\sigma]' + \sigma'' - 2\alpha\sigma, \end{aligned} \quad (\text{A2})$$

where  $\rho = (\rho_+ + \rho_-)/2$  and  $\sigma = (\rho_+ - \rho_-)/2$ . From the first equation we get  $z\sigma = -z\rho - 2\rho' + \text{const}$ , where  $\text{const} = 0$  as a result of the even symmetry of  $\rho(z)$ . From this we can generate a sequence of expressions

$$\begin{aligned} \sigma &= -\rho - \frac{2}{z}\rho', \\ \sigma' &= -\rho' + \frac{2}{z^2}\rho' - \frac{2}{z}\rho'', \\ \sigma'' &= -\rho'' - \frac{4}{z^3}\rho' + \frac{4}{z^2}\rho'' - \frac{2}{z}\rho'''. \end{aligned} \quad (\text{A3})$$

Inserting these expressions into the second equation in Eq. (A2) recovers Eq. (4).

**APPENDIX B: RECURRENCE RELATION**

In this section we show how to obtain even moments, defined as

$$\langle z^{2n} \rangle_{\pm} = \int_{-\infty}^{\infty} dz z^{2n} \rho_{\pm}(z),$$

from the two equations in Eq. (3), which we repeat below for clarity:

$$\begin{aligned} 0 &= [z\rho_+] + \rho_+'' + \alpha(\rho_- - \rho_+) \\ 0 &= \rho_-'' + \alpha(\rho_+ - \rho_-). \end{aligned} \quad (\text{B1})$$

To convert the two equations into the recurrence relation, we operate on both equation with  $\int_{-\infty}^{\infty} dz z^{2n+2}$ . This results in the following two coupled recurrence relations:

$$\begin{aligned} 0 &= -(2n+2)m_{n+1}^+ + (2n+2)(2n+1)m_n^+ \\ &\quad + \alpha(m_{n+1}^- - m_{n+1}^+) \\ 0 &= (2n+2)(2n+1)m_n^- + \alpha(m_{n+1}^+ - m_{n+1}^-), \end{aligned} \quad (\text{B2})$$

where  $m_n^+ = \langle z^{2n} \rangle_+$  and  $m_n^- = \langle z^{2n} \rangle_-$ . After rearrangement, the two equations become

$$\begin{aligned} m_{n+1}^+ &= (2n+1)(m_n^+ + m_n^-) \\ m_{n+1}^+ &= (2n+1)(m_n^+ - m_n^-) - \frac{2\alpha}{(2n+2)}(m_{n+1}^+ - m_{n+1}^-). \end{aligned}$$

The initial terms of both sequences are  $m_0^+ = m_0^- = 1$ . The remaining terms can be obtained from the recurrence relations above.

**APPENDIX C: DERIVATION OF EQ. (12)**

In this section we demonstrate how combining the two equations in Eq. (12), which we reproduce below:

$$\begin{aligned} 0 &= [\lambda(\lambda-1)p_+] + \frac{\alpha}{2}(p_- - p_+) \\ 0 &= [\lambda^2 p_-]' + \frac{\alpha}{2}(p_+ - p_-), \end{aligned} \quad (\text{C1})$$

yields Eq. (15). Adding and subtracting the two equations yields

$$\begin{aligned} 0 &= [\lambda(2\lambda-1)p]' - \lambda\sigma' \\ 0 &= 2[\lambda^2\sigma]' - \lambda p' - \lambda\sigma' - 2\alpha\sigma, \end{aligned} \quad (\text{C2})$$

where  $p = (p_+ + p_-)/2$  and  $\sigma = (p_+ - p_-)/2$ . From the first equation we get  $\sigma = (2\lambda-1)p$  and from which we generate the consecutive expressions

$$\begin{aligned} \sigma &= (2\lambda-1)p, \\ \sigma' &= 2p + (2\lambda-1)p', \end{aligned} \quad (\text{C3})$$

Inserting these expressions into the second equation in Eq. (C2) recovers Eq. (15).

**APPENDIX D: DERIVATION OF  $\langle v^2 \rangle$** 

In Sec. (VIC) in Eq. (45) we provide an expression for the dissipation of heat which includes the quantity  $\langle v^2 \rangle$ . To calculate  $\langle v^2 \rangle$  we formulate the problem within underdamped dynamics, which will take us slightly beyond the objectives of the present work.

To begin with, we formulate the problem within the Kramer's equation, which is the type of a Fokker-Planck equation but that includes inertia [53],

$$\begin{aligned} \frac{\partial \rho_+}{\partial t} &= -\mathbf{v} \cdot \nabla_r \rho_+ + \frac{1}{\tau_r} \nabla_v \cdot [(\mu K \mathbf{r} + \mathbf{v}) \rho_+] \\ &\quad + \frac{D}{\tau_r^2} \nabla_v^2 \rho_+ + \frac{1}{\tau} (\rho_- - \rho_+) \\ \frac{\partial \rho_-}{\partial t} &= -\mathbf{v} \cdot \nabla_r \rho_- + \frac{1}{\tau_r} \nabla_v \cdot [\mathbf{v} \rho_-] \\ &\quad + \frac{D}{\tau_r^2} \nabla_v^2 \rho_- + \frac{1}{\tau} (\rho_+ - \rho_-), \end{aligned}$$

where  $\rho_{\pm} \equiv \rho_{\pm}(\mathbf{r}, \mathbf{v}, t)$ , and we recall that  $\tau_r = m\mu$  is the inertial relaxation,  $m$  is a particle mass, and the overdamped regime is recovered for  $\tau_r = 0$ .

To calculate  $\langle v^2 \rangle$ , or other average quantities of interest, we operate on the stationary Kramer's equation,  $\dot{\rho} = 0$ , with an integral operator  $\hat{O}_g = \int d\mathbf{v} \int d\mathbf{r} g(\mathbf{r}, \mathbf{v})$ , where the function  $g$  is going to be defined later. Using integration by parts, the terms of a transformed Kramer's equation can be represented as average quantities, designated by the angular brackets  $\langle \dots \rangle = \int d\mathbf{v} \int d\mathbf{r} (\dots)$ . The resulting two equations

are

$$0 = \langle \mathbf{v} \cdot \nabla_r g \rangle_+ - \frac{1}{\tau_r} \langle (\mu K \mathbf{r} + \mathbf{v}) \cdot \nabla_v g \rangle_+ + \frac{D}{\tau_r^2} \langle \nabla_v^2 g \rangle_+ \\ + \frac{\langle g \rangle_-}{\tau} - \frac{\langle g \rangle_+}{\tau} \\ 0 = \langle \mathbf{v} \cdot \nabla_r g \rangle_- - \frac{1}{\tau_r} \langle \mathbf{v} \cdot \nabla_v g \rangle_- + \frac{D}{\tau_r^2} \langle \nabla_v^2 g \rangle_- \\ + \frac{\langle g \rangle_+}{\tau} - \frac{\langle g \rangle_-}{\tau}.$$

Using  $g = v^2$ ,  $g = r^2$ , and  $g = \mathbf{r} \cdot \mathbf{v}$ , we generate from the relation above six equations involving six unknown average quantities,

$$0 = -\frac{2}{\tau_r} \langle v^2 \rangle_+ + \frac{2dD}{\tau_r^2} - \frac{1}{\tau} \langle v^2 \rangle_+ + \frac{1}{\tau} \langle v^2 \rangle_- - \frac{2\mu K}{\tau_r} \langle \mathbf{r} \cdot \mathbf{v} \rangle_+ \\ 0 = -\frac{2}{\tau_r} \langle v^2 \rangle_- + \frac{2dD}{\tau_r^2} - \frac{1}{\tau} \langle v^2 \rangle_- + \frac{1}{\tau} \langle v^2 \rangle_+ \\ 0 = \langle v^2 \rangle_+ + \frac{1}{\tau_r} \langle \mathbf{v} \cdot \mathbf{r} \rangle_+ - \frac{1}{\tau} \langle \mathbf{v} \cdot \mathbf{r} \rangle_+ + \frac{1}{\tau} \langle \mathbf{v} \cdot \mathbf{r} \rangle_- \\ - \frac{\mu K}{\tau_r} \langle r^2 \rangle_+$$

$$0 = \langle v^2 \rangle_- - \frac{1}{\tau_r} \langle \mathbf{v} \cdot \mathbf{r} \rangle_- - \frac{1}{\tau} \langle \mathbf{v} \cdot \mathbf{r} \rangle_- + \frac{1}{\tau} \langle \mathbf{v} \cdot \mathbf{r} \rangle_+ \\ 0 = 2 \langle \mathbf{v} \cdot \mathbf{r} \rangle_+ - \frac{1}{\tau} \langle r^2 \rangle_+ + \frac{1}{\tau} \langle r^2 \rangle_- \\ 0 = 2 \langle \mathbf{v} \cdot \mathbf{r} \rangle_- - \frac{1}{\tau} \langle r^2 \rangle_- + \frac{1}{\tau} \langle r^2 \rangle_+. \quad (\text{D1})$$

After solving the above system of coupled equations, we get

$$\langle v^2 \rangle - \frac{dD}{\tau_r} = -\frac{d\tau D \mu K (\tau_r + \tau)}{\mu K \tau_r^2 \tau - 4\tau_r^2 - 6\tau_r \tau - 2\tau^2}, \quad (\text{D2})$$

which for the overdamped regime  $\tau_r = 0$  reduces to

$$\langle v^2 \rangle - \frac{dD}{\tau_r} = \frac{dD \mu K}{2}. \quad (\text{D3})$$

Since  $\langle v^2 \rangle_{\text{eq}} = \frac{dD}{\tau_r}$ , and since  $\langle v^2 \rangle$  is proportional to the kinetic energy, we can think of the above quantity as representing the excess kinetic energy that arises due to fluctuations of a harmonic trap.

- 
- [1] J. Tailleur and M. E. Cates, Statistical mechanics of interacting run-and-tumble bacteria, *Phys. Rev. Lett.* **100**, 218103 (2008).
- [2] J. Tailleur and M. E. Cates, Sedimentation, trapping, and rectification of dilute bacteria, *Europhys. Lett.* **86**, 60002 (2009).
- [3] M. R. Evans and S. N. Majumdar, Run and tumble particle under resetting: A renewal approach, *J. Phys. A: Math. Theor.* **51**, 475003 (2018).
- [4] K. Malakar, V. Jemseena, A. Kundu, K. V. Kumar, S. Sabhapandit, S. N. Majumdar, S. Redner, and A. Dhar, Steady state, relaxation and first-passage properties of a run-and-tumble particle in one-dimension, *J. Stat. Mech.: Theory Exp.* (2018) 043215.
- [5] A. Dhar, A. Kundu, S. N. Majumdar, S. Sabhapandit, and G. Schehr, Run-and-tumble particle in one-dimensional confining potentials: Steady-state, relaxation, and first-passage properties, *Phys. Rev. E* **99**, 032132 (2019).
- [6] U. Basu, S. N. Majumdar, A. Rosso, S. Sabhapandit, and G. Schehr, Exact stationary state of a run-and-tumble particle with three internal states in a harmonic trap, *J. Phys. A: Math. Theor.* **53**, 09LT01 (2020).
- [7] A. Villa-Torrealba, C. Chávez-Raby, P. de Castro, and R. Soto, Run-and-tumble bacteria slowly approaching the diffusive regime, *Phys. Rev. E* **101**, 062607 (2020).
- [8] N. Razin, Entropy production of an active particle in a box, *Phys. Rev. E* **102**, 030103(R) (2020).
- [9] D. Frydel, Generalized run-and-tumble model in 1D geometry for an arbitrary distribution of drift velocities, *J. Stat. Mech. Theory Exp.* (2021) 083220.
- [10] D. Frydel, Kuramoto model with run-and-tumble dynamics, *Phys. Rev. E* **104**, 024203 (2021).
- [11] N. R. Smith and O. Farago, Nonequilibrium steady state for harmonically confined active particles, *Phys. Rev. E* **106**, 054118 (2022).
- [12] D. Frydel, The four-state RTP model: Exact solution at zero temperature, *Phys. Fluids* **34**, 027111 (2022).
- [13] C. Roberts and Z. Zhen, Run-and-tumble motion in a linear ratchet potential: Analytic solution, power extraction, and first-passage properties, *Phys. Rev. E* **108**, 014139 (2023).
- [14] O. Farago and N. R. Smith, Confined run-and-tumble particles with non-Markovian tumbling statistics, *Phys. Rev. E* **109**, 044121 (2024).
- [15] T. Pietrangeli, C. Ybert, C. Cottin-Bizonne, and F. Detcheverry, Optimal run-and-tumble in slit-like confinement, *Phys. Rev. Res.* **6**, 023028 (2024).
- [16] B. Loewe, T. Kozhukhov, and T. N. Shendruk, Anisotropic run-and-tumble-turn dynamics, *Soft Matter* **20**, 1133 (2024).
- [17] K. Malakar, A. Das, A. Kundu, K. V. Kumar, and A. Dhar, Steady state of an active Brownian particle in a two-dimensional harmonic trap, *Phys. Rev. E* **101**, 022610 (2020).
- [18] M. Caraglio and T. Franosch, Analytic solution of an active Brownian particle in a harmonic well, *Phys. Rev. Lett.* **129**, 158001 (2022).
- [19] G. Szamel, Self-propelled particle in an external potential: Existence of an effective temperature, *Phys. Rev. E* **90**, 012111 (2014).
- [20] S. Shankar and M. C. Marchetti, Hidden entropy production and work fluctuations in an ideal active gas, *Phys. Rev. E* **98**, 020604(R) (2018).
- [21] F. J. Sevilla, R. F. Rodríguez, and J. R. Gomez-Solano, Generalized Ornstein-Uhlenbeck model for active motion, *Phys. Rev. E* **100**, 032123 (2019).

- [22] D. Martin, J. O'Byrne, M. E. Cates, É. Fodor, C. Nardini, J. Tailleur, and F. van Wijland, Statistical mechanics of active Ornstein-Uhlenbeck particles, *Phys. Rev. E* **103**, 032607 (2021).
- [23] L. Caprini, U. M. B. Marconi, and A. Vulpiani, Linear response and correlation of a self-propelled particle in the presence of external fields, *J. Stat. Mech.: Theory Exp.* (2018) 033203.
- [24] G. H. Philipp Nguyen, Active Ornstein-Uhlenbeck model for self-propelled particles with inertia, *J. Phys.: Condens. Matter* **34**, 035101 (2022).
- [25] A. Pal and S. Sabhapandit, Work fluctuations for a Brownian particle in a harmonic trap with fluctuating locations, *Phys. Rev. E* **87**, 022138 (2013).
- [26] Z. Zhang and W. Wang, The stationary distribution of Ornstein-Uhlenbeck process with a two-state Markov switching, *Commun. Stat. Simul. Comput.* **46**, 4783 (2017).
- [27] I. Santra, S. Das, and S. K. Nath, Brownian motion under intermittent harmonic potentials, *J. Phys. A: Math. Theor.* **54**, 334001 (2021).
- [28] D. Gupta, A. Pal, and A. Kundu, Resetting with stochastic return through linear confining potential, *J. Stat. Mech: Theory Exp.* (2021) 043202.
- [29] D. Gupta, C. A. Plata, A. Kundu, and A. Pal, Stochastic resetting with stochastic returns using external trap, *J. Phys. A: Math. Theor.* **54**, 025003 (2021).
- [30] H. Alston, L. Cocconi, and T. Bertrand, Non-equilibrium thermodynamics of diffusion in fluctuating potentials, *J. Phys. A: Math. Theor.* **55**, 274004 (2022).
- [31] Y. Sokolov, D. Frydel, D. G. Grier, H. Diamant, and Y. Roichman, Hydrodynamic pair attractions between driven colloidal particles, *Phys. Rev. Lett.* **107**, 158302 (2011).
- [32] S. C. Takatori, R. De Dier, J. Vermant, and J. F. Brady, Acoustic trapping of active matter, *Nat. Commun.* **7**, 10694 (2016).
- [33] R. Goerlich, M. Li, S. Albert, G. Manfredi, P. A. Hervieux, and C. Genet, Noise and ergodic properties of Brownian motion in an optical tweezer: Looking at regime crossovers in an Ornstein-Uhlenbeck process, *Phys. Rev. E* **103**, 032132 (2021).
- [34] I. Buttinoni, L. Caprini, L. Alvarez, F. J. Schwarzendahl, and H. Löwen, Active colloids in harmonic optical potentials, *Europhys. Lett.* **140**, 27001 (2022).
- [35] R. Goerlich, L. B. Pires, G. Manfredi, P. A. Hervieux, and C. Genet, Harvesting information to control nonequilibrium states of active matter, *Phys. Rev. E* **106**, 054617 (2022).
- [36] O. Chor, A. Sohachi, R. Goerlich, E. Rosen, S. Rahav, and Y. Roichman, Many-body Szilárd engine with giant number fluctuations, *Phys. Rev. Res.* **5**, 043193 (2023).
- [37] D. Frydel, Positing the problem of stationary distributions of active particles as third-order differential equation, *Phys. Rev. E* **106**, 024121 (2022).
- [38] D. Frydel, Run-and-tumble oscillator: Moment analysis of stationary distributions, *Phys. Fluids* **35**, 101905 (2023).
- [39] D. Frydel, Active oscillator: Recurrence relation approach, *Phys. Fluids* **36**, 011910 (2024).
- [40] H. Kleinert, *Path Integrals in Quantum Mechanics, Statistics, Polymer Physics and Financial Markets* (World Scientific, Singapore, 2004).
- [41] P. Jizba and H. Kleinert, Superpositions of probability distributions, *Phys. Rev. E* **78**, 031122 (2008).
- [42] C. Beck, Dynamical foundations of nonextensive statistical mechanics, *Phys. Rev. Lett.* **87**, 180601 (2001).
- [43] J. M. Parrondo, J. M. Horowitz, and T. Sagawa, Thermodynamics of information, *Nat. Phys.* **11**, 131 (2015).
- [44] T. Sagawa and M. Ueda, Second law of thermodynamics with discrete quantum feedback control, *Phys. Rev. Lett.* **100**, 080403 (2008).
- [45] F. J. Cao and M. Feito, Thermodynamics of feedback controlled systems, *Phys. Rev. E* **79**, 041118 (2009).
- [46] J. M. Horowitz and S. Vaikuntanathan, Nonequilibrium detailed fluctuation theorem for repeated discrete feedback, *Phys. Rev. E* **82**, 061120 (2010).
- [47] T. Sagawa and M. Ueda, Generalized Jarzynski equality under nonequilibrium feedback control, *Phys. Rev. Lett.* **104**, 090602 (2010).
- [48] M. Ponmurugan, Generalized detailed fluctuation theorem under nonequilibrium feedback control, *Phys. Rev. E* **82**, 031129 (2010).
- [49] Y. Fujitani and H. Suzuki, Jarzynski equality modified in the linear feedback system, *J. Phys. Soc. Jpn.* **79**, 104003 (2010).
- [50] A. Kundu, Nonequilibrium fluctuation theorem for systems under discrete and continuous feedback control, *Phys. Rev. E* **86**, 021107 (2012).
- [51] J. R. Gomez-Solano, L. Bellon, A. Petrosyan, and S. Ciliberto, Steady-state fluctuation relations for systems driven by an external random force, *Europhys. Lett.* **89**, 60003 (2010).
- [52] S. Padhi and S. Pati, *Theory of Third-Order Differential Equations* (Springer Science and Business Media, New York, 2013).
- [53] D. Frydel, Entropy production of active particles formulated for underdamped dynamics, *Phys. Rev. E* **107**, 014604 (2023).
- [54] P. Sartori, E. Chiarello, G. Jayaswal, M. Pierno, G. Mistura, P. Brun, A. Tiribocchi, and E. Orlandini, Wall accumulation of bacteria with different motility patterns, *Phys. Rev. E* **97**, 022610 (2018).